On the Severity of Wind Turbine Generator Speed Peaks in Response to Particular Gusts*

Mandar Phadnis[1] and Lucy Pao[2]

***Abstract*— An objective of a wind turbine control system is to avoid generator over-speeds that can trigger turbine shutdown. This work aims to study the wind and the control actuator signals for a two-bladed downwind turbine to assess generator speed peaking behavior. Peaks in generator speed are often observed when there is a lull in wind speed followed by a rising gust. A 'gust measure' is used to quantify the severity of such peaks. Field data from the Segmented Ultralight Morphing Rotor demonstrator turbine tested at the US National Renewable Energy Laboratory is used for this assessment. Nacelle wind speed is analyzed for simulation and field cases to determine a gust measure for particular sequences of wind inputs preceding peaks in generator speed. The gust measure tested under varied wind conditions to estimate peaks in generator speed shows a good correlation between high values of the gust measure and peak occurrences in generator speed. A novel modified gust measure that accounts for the proximity to a control transition from region 2 torque control to region 3 blade pitch control is developed to further improve the correlation. We conclude that gust measures of the forms described here can be used online with advanced control strategies to predict and mitigate generator speed peaks.**

I. INTRODUCTION

Wind turbine controllers deal with a complex task of maximizing power production while simultaneously maintaining safe operation for the turbine [1]. One of the constraints for a wind turbine is the maximum allowable speed its generator can operate at before necessitating a shutdown [2]. A shutdown procedure takes a wind turbine out of power production, causing loss of revenue and increase in the levelized cost of energy (LCOE) [3]. Generator speed regulation away from the shutdown threshold is therefore a goal of a wind turbine controller. Generally this threshold is approximately 20% above the rated speed of the generator [4].

The main control objective for a turbine is decided by its operating region [1]. In below-rated operation, the turbine control maximizes power capture from the wind using generator torque actuation, whereas in above-rated conditions it regulates power to rated capacity by modulating the aerodynamic torque on the rotor by pitching the blades.

Under normal operating conditions, generator torque control and blade pitch control modes work in their respective operating regions to optimize power capture while constraining structural loads on the turbine. This is complicated by turbulence in the wind, which causes fluctuations in the power, generator speed, and mechanical loading. The turbulence can also result in the control modes switching back and forth due to rapid changes in the wind. There are control strategies developed to reduce the ill-effects of such switching [5,6]. In particular, if there is a drop in the wind speed followed by a rising gust, the control may switch from blade pitch to generator torque and back to blade pitch in a relatively short period, adversely affecting the generator speed. We observe that under particular patterns in the inflow wind, where a lull in the wind speed is followed by a rising gust, the generator speed response shows a peaking behavior. While being generally undesirable, the peaks in generator speed may also violate the turbine shutdown threshold, resulting in a shutdown and loss of power generation [3].

The turbine model used for the analysis in this work was developed as part of the 'Segmented Ultralight Morphing Rotor' (SUMR) project [7], which was funded by the US Department of Energy [8,9]. This project has designed a 50 MW 2-bladed downwind concept rotor called SUMR-50. Earlier iterations of 13.2 MW turbine (SUMR-13) designs showed potential for reduced rotor mass, capital costs, and LCOE [10]. To validate these design results, an experimental test campaign was undertaken to manufacture a scaled SUMR-13 based demonstrator rotor for field testing. Since construction costs of a 13.2 MW turbine would be exorbitant, an aero-gravo-elastically down-scaled model was designed [11,12]. The down-scaled 53.38 kW turbine called SUMR-Demonstrator (SUMR-D) was manufactured, deployed and tested extensively on the National Renewable Energy Laboratory's (NREL's) 2-bladed Controls Advanced Research Turbine (CART2) [13]. The data from this demonstration [9] provided an opportunity to evaluate the correlations between particular wind gust patterns with generator speed peaks under field conditions.

A 'gust measure' developed in [3] is used to quantify such wind gusts as a way to predict a generator speed peak occurrence. The correlation between the gust measure and the severity of wind speed peaks is studied. Wind conditions from the field test are replicated using TurbSim [14] for use in fully nonlinear aero-elastic simulations within the OpenFAST framework [15]. Having similar conditions for

*This work was supported in part by the Advanced Research Projects Agency - Energy (ARPA-e) ATLANTIS Program, under Award Number DE-AR0000667. Any opinions, findings, and conclusions or recommendations expressed in this material are those of the authors and do not necessarily reflect the views of ARPA-e. We would also like to thank Daniel Zalkind for discussions on wind gust measures as well as Lee Jay Fingersh, Andrew Scholbrock, and the team at NREL for conducting the SUMR-D field test, gathering and organizing the data, and making it available for analysis.

[1]Mandar Phadnis is a graduate student in Aerospace Engineering Sciences, University of Colorado Boulder, Boulder, CO, USA mandar.phadnis@colorado.edu

[2]Lucy Pao is a Professor with the Department of Electrical, Computer, and Energy Engineering, University of Colorado Boulder, Boulder, CO, USA lucy.pao@colorado.edu

TABLE I: SUMR-D Turbine Parameters

Blade length (m)	20.919
No. of blades (-)	2
Hub height (m)	36.6
Pre-cone angle (deg)	12.5
Rotor radius (m)	22.6
Rated power (kW)	53.38
Rated generator speed (RPM)	926.7525
Rated torque (Nm)	550
Rated wind speed (m/s)	5.0535

simulation and field cases allows for a validation of the gust measure that is tuned for a simulated model and 'tested' under field conditions. As a novel contribution of this work, the gust measure is then modified to account for the likelihood of a wind sequence causing the controller to switch modes, resulting in more severe generator speed peaks. The modified gust measure is observed to improve the correlation for both simulated and field cases. The (modified) gust measure(s) can ultimately be used online in control loops to mitigate undesirable peaks in generator speed.

This paper is organized as follows. The turbine configuration and control structure are described in Section II. The gust measure is explained in Section III and the modified gust measure is developed in Section IV. Replication of field wind conditions for representative simulations is covered in Section V, along with the results of the analysis. Section VI provides discussion and conclusions.

II. SUMR-D Model and Controller

A. Turbine Configuration

SUMR-D was an aero-gravo-elastically down-scaled 53.38 kW rotor that was field tested at NREL on the CART2 platform. Details of the CART2 system and the down-scaling methodology used for SUMR-D can be found in [16] and [12,17], respectively. The upwind, 600 kW CART2 system was modified to a downwind, highly coned configuration and de-rated to 53.38 kW operation for the SUMR-D campaign [13]. The SUMR-D consists of two blades with a 22.6 meter rotor radius at a hub height of 36.6 meters. It has cut-in, rated, and cut-out wind speeds of 3 m/s, 5.05 m/s, and 11 m/s, respectively. The relevant turbine parameters are noted in Table I.

B. Turbine Control

At very low wind speeds, where the turbine losses exceed the power available in the wind, the turbine is not operated (region 1). After a certain cut-in wind speed, the turbine operates below its rated capacity (region 2), where the primary goal of the controller is to maximize power generation by actuating the generator torque to optimal values; the turbine blades are at a designed "fine pitch angle" to maximize the aerodynamic torque on the rotor. At higher wind speeds, the wind power available is higher than the turbine's rated capacity (region 3). The main control objective for region 3 is to maintain the power produced at rated power by pitching the blades to manipulate the aerodynamic torque on the rotor; the generator torque is usually held at a constant rated torque.

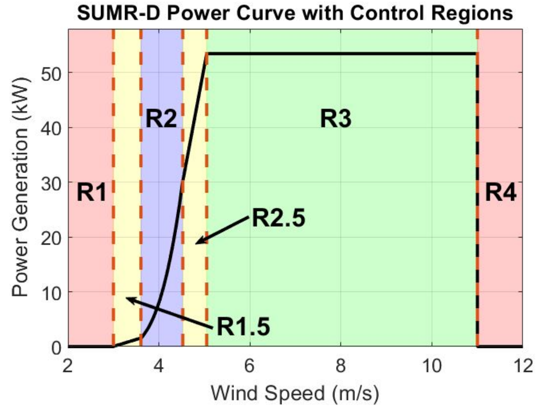

Fig. 1: SUMR-D Power Curve with Control Regions: R1 and R4 (red) are pre cut-in and post cut-out, R2 (blue) is below rated, R3 (green) is above rated, and R1.5 and R2.5 (yellow) are linear transition regions. The black curve shows ideal power capture as a function of wind speed.

At even higher wind speeds, the aerodynamic loads on the wind turbine components become too large for safe operation and the turbine is shutdown (region 4).

Fig. 1 shows the ideal power capture curve for SUMR-D as a function of wind speed along with the control regions described above. The regions below cut-in (R1) and beyond cut-out (R4) wind speeds are marked in red, where no power is produced. The below-rated operational region 2, where power capture is maximized using torque control is marked blue. The above-rated operational region 3, where the power produced is regulated at rated power using blade pitch control is marked green, with the transition regions (R1.5 and R2.5) marked yellow. As shown in Fig. 2, in region 2, the SUMR-D controller employs the so called $K\omega^2$ nonlinear torque control law [1] to maximize power capture, with linear torque control set-points in the transition region between regions 2 and 3 [18]. In region 3, SUMR-D uses a gain-scheduled Proportional-Integral (PI) collective blade pitch control to regulate the generator speed at rated RPM. A detailed development of the blade pitch and generator torque controllers used for SUMR-D can be found in [7]. It is important to note that the control did not include a set-point smoothing feature [6] that is sometimes used to reduce generator speed fluctuations in near-rated operation under turbulent wind conditions.

III. Gust Measure

The SUMR-D rotor on the CART2 platform had multiple wind sensors available. Of those, the nacelle cup anemometer measuring wind speed at the rotor is used in the following analysis to calculate the gust measure. Being a downwind rotor, this measurement taken upstream from the turbine, is more reliable for SUMR-D analysis than it is for traditional upwind configurations.

The gust measure from [3] is briefly summarized here and implemented on the SUMR-D field data and simulations. A window of wind speeds is used:

$$U_{window} = \{u(t - t_r)\}_{r=0,\ldots,N} \tag{1}$$

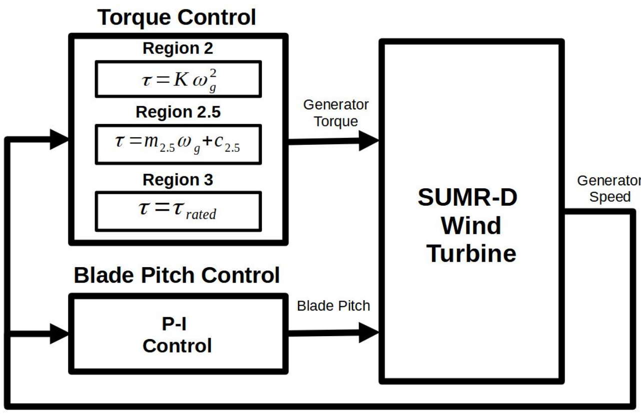

Fig. 2: SUMR-D Controller Structure

where $u(t_i)$ is the wind speed at time t_i and a history of N past wind speeds are used. The time delays

$$t_r = r\Delta t \tag{2}$$

are spaced Δt seconds apart. A set of weighted differences between the current wind speed $u(t)$ and the delayed wind speeds is calculated:

$$\Delta U_{window} = \{w_{ur}[u(t) - u(t - t_r)]\}_{r=0,\dots,N} \tag{3}$$

where linear weights prioritize more recent samples:

$$w_{ur} = \frac{r}{N} + \left(1 - \frac{r}{N}\right) w_{u0}, \qquad r = 0, \dots, N \tag{4}$$

with $w_{u0} > 1$ being the highest weight given to the current wind speed $u(t)$ and decreasing to $w_{ur} = 1$ when $r = N$.

The maximum of the weighted differences is taken as the gust measure δu_0 [3]:

$$\delta u_0 = \max_r \{\Delta U_{window}\} \tag{5}$$

It has been observed that there is often a time delay between the peak of the wind gust and the peak seen in generator speed. For the gust measure to accurately account for this delay, the calculation in equation (5) is repeated at 1 second intervals going back 4 seconds from the generator speed peak occurrence. The gust measure accounting for delay δU_d is taken to be the maximum of these five iterations:

$$\delta U_d = \max_i \{\delta u_i\}_{i=0,\dots,4} \tag{6}$$

IV. Modified Gust Measure

It has been observed that the severity of peaks in generator speed is greater if the control is transitioning from region 2 to region 3. This is due to switching of the control actuation from torque control to blade pitch control, with the generator speed near its rated RPM. However, the gust measure as presented above only takes into account the nature of the wind input. In order to improve the correlation between the gust measure and the generator speed peak, we can also account for the proximity of the control to the transition. This can be achieved by applying a similar algorithm to the generator torque signal which accounts for any rise in generator torque towards its saturation limit at rated torque, where the control switches to pitch control in region 3. Using a window of generator torque samples similar to that applied to the wind signal in equation (1), we have:

$$\tau_{window} = \{\tau(t - t_r)\}_{r=0,\dots,N} \tag{7}$$

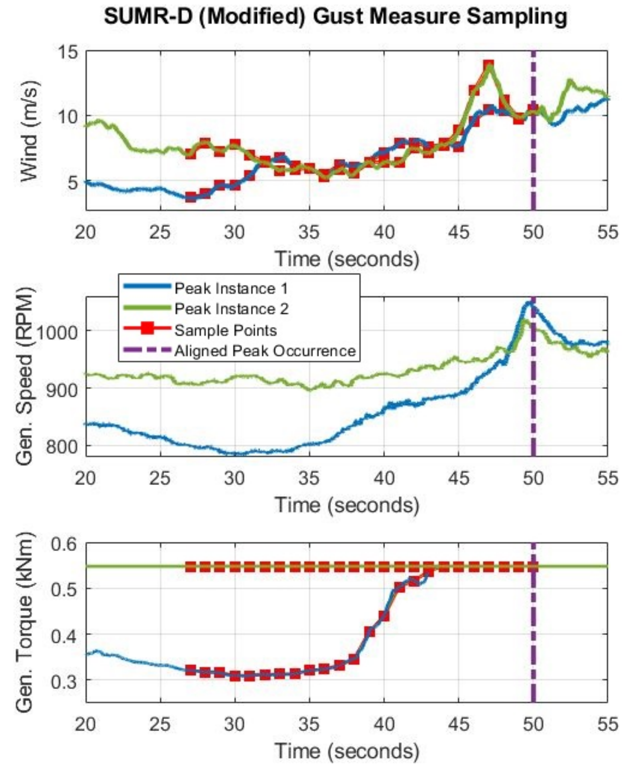

Fig. 3: Sampling of wind speed and generator torque for Modified Gust Measure δG_d. For Peak Instance 1, the modified gust measure δG_d is greater than the gust measure δU_d due to the proximity to a control transition, whereas for Peak Instance 2 both measures are the same since the period leading up to the peak occurs purely in region 3.

Examples of wind speed and generator torque sampling are shown in Fig. 3. Using similar weighted differences as seen in equations (2)-(5), we obtain a 'torque measure' $\delta\tau_0$:

$$\delta\tau_0 = \max_r \{\Delta\tau_{window}\} \tag{8}$$

Iterating over the previous 4 seconds, the torque measure accounting for delay $\delta\tau_d$ is obtained:

$$\delta\tau_d = \max_i \{\delta\tau_i\}_{i=0,\dots,4} \tag{9}$$

The Gust Measure as shown in equation (6) can then be modified as the weighted sum of the gust measure accounting for delay and the torque measure accounting for delay:

$$\delta G_d = k_U \delta U_d + k_\tau \delta\tau_d \tag{10}$$

where k_U and k_τ are weighting parameters.

These measures are listed in Table II, and the tuning parameters for the modified gust measure are summarized in Table III. Proper tuning of the parameters would be crucial for an online implementation of the (modified) gust measure within a controller to reduce generator speed peaks.

TABLE II: Summary of Measures

Measures	Equation	Notes
δu_0	Eq. (5)	Gust Measure developed in [3]
δU_d	Eq. (6)	Gust Measure accounting for delay
$\delta \tau_0$	Eq. (8)	Torque Measure for proximity to transition
$\delta \tau_d$	Eq. (9)	Torque Measure accounting for delay
δG_d	Eq. (10)	Modified Gust Measure

TABLE III: (Modified) Gust Measure Tuning Parameters

Number of samples	N	20
Sampling Period	Δt	1 second
Highest weight for wind samples	w_{u0}	2.5 (m/s)$^{-1}$
Highest weight for generator torque samples	$w_{\tau 0}$	45 (kNm)$^{-1}$
Weight for gust measure	k_U	1
Weight for torque measure	k_τ	0.55

TABLE IV: SUMR-D Wind Sensor Locations

Sensor	Height (m)	Upstream Distance (m)
Nacelle cup anemometer	36.6	0
Met mast cup anemometer 1	3	40
Met mast cup anemometer 2	15	40
Met mast cup anemometer 3	36	40
Met mast cup anemometer 4	58	40
Met mast sonic anemometer	36.6	40

V. RESULTS

The performance of the (modified) gust measure(s) is analyzed using generator speed and torque signals from simulations of the SUMR-D model in NREL's OpenFAST [15] tool and SUMR-D field test data. The field datasets were replicated as closely as possible in OpenFAST using TurbSim version 2 [14] to generate wind files representing the field conditions. This allows us to tune the gust measures for a simulated model and validate its performance using the field data. The nacelle anemometer as well as cup anemometers and a sonic anemometer on a met mast are the SUMR-D field sensors used to generate simulated wind fields to match the field conditions. Due to the downwind configuration, the nacelle anemometer is upwind of the rotor and hence less susceptible to axial induction bias effects as compared to a conventional upwind rotor. The nacelle anemometer at the hub height of 36.6 m is given as a reference time-series to TurbSim, to generate wind inputs along the downwind u-axis. Cup anemometers at heights of 3 m, 15 m, 36 m, and 58 m on a met mast were used to calculate mean vertical shear, whereas the sonic anemometer on the met mast is used to provide the normal distribution to generate wind along the transverse v and w axes. The sensors and their locations are summarized in Table IV. Though multiple wind sensors are available, it is still not possible to measure all of the higher frequency turbulence information across the rotor plane. In addition, there are differences between the modeled blades, pitch actuators, generator, etc. and the actual components. As such, the exact wind turbine response cannot be reproduced in simulation. For this study, we selected the best matches that were observed between the field data and representative simulations in OpenFAST. An example of such a dataset is shown in Fig. 4.

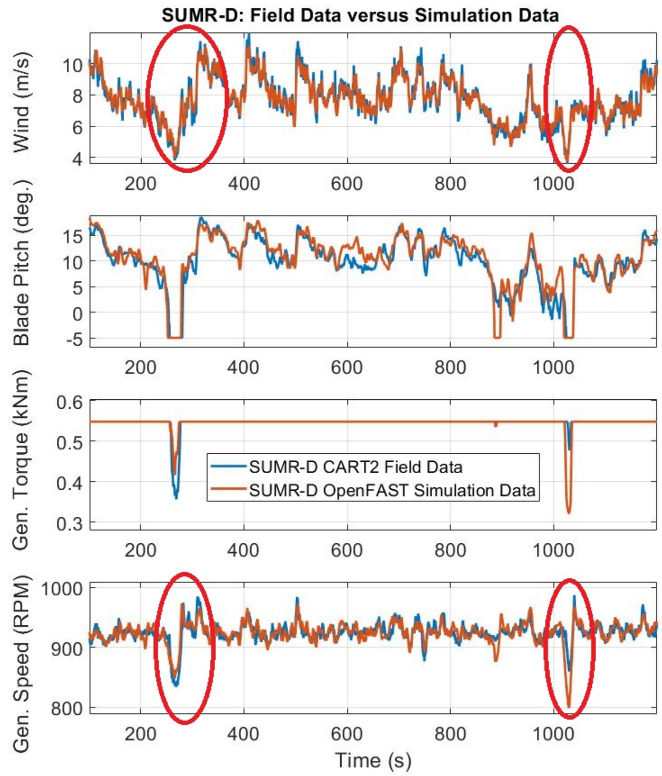

Fig. 4: Field data and representative simulation case for the SUMR-D turbine. Circled are instances of particular wind gusts causing the generator speed to peak. The first 100 seconds are removed to avoid OpenFAST transients.

A. *Particular Gust Trends*

A lull in wind followed by a rising positive gust is observed to cause a peak in generator speed response. The gust measure in Section III was developed to gauge such occurrences. Further, the severity of the peak is seen to be higher if the control switches from region 2 to region 3 during this particular gust. A look at the ensemble trend in proximity of these generator speed peaks gives us an initial insight into this behavior.

To detect the peaks, the generator speed signal is filtered using a moving average over a span of 2 seconds, to remove the high-frequency noise. The local maxima above a certain threshold in generator speed peaks are considered. In Fig. 5, we take the top 30 generator speed peak occurrences for each: those over 972 RPM from SUMR-D simulations (faint red) and those over 985 RPM from SUMR-D field data (faint blue) and align them such that every peak occurs at $t_{peak} = 50$ seconds. We look at the preceding 50 seconds and following 10 seconds of each instance. We can gain insight from the wind, generator speed, blade pitch angle, and generator torque signals. As shown in Fig. 5, an ensemble average across time for the aligned peak instances shows a trend. The wind speed on average shows a lull followed by a positive gust with a corresponding dip, rise, peak, and drop in the generator speed. The blade pitch and generator torque actuator signals show that, on average, the control is in region 2 before the peak and in region 3 after the peak. This is clear

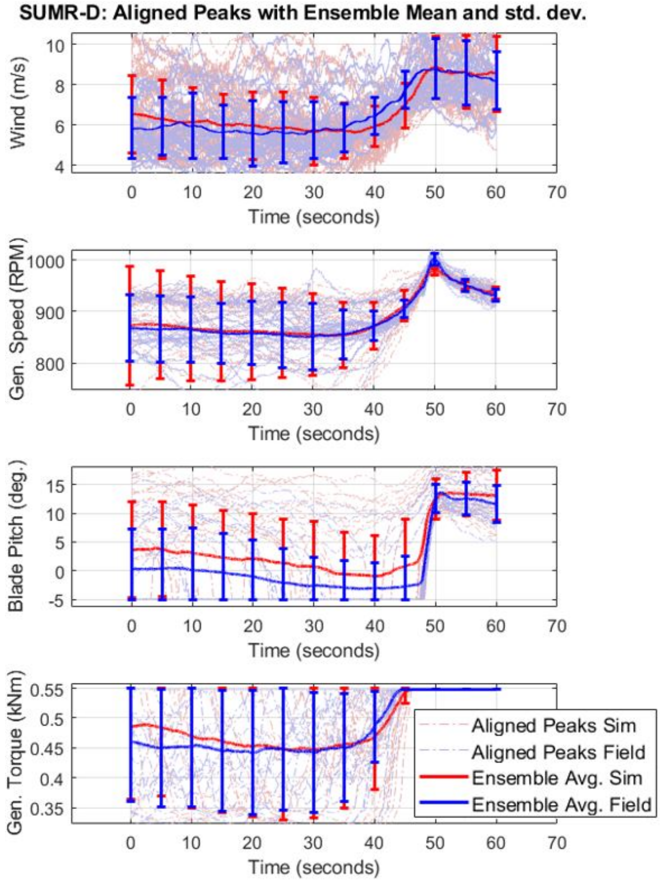

Fig. 5: Ensemble trend for highest 30 generator speed peak occurrences aligned at 50 second mark for SUMR-D simulation and field data

from the ensemble average generator torque saturating just before the 50 second mark.

B. *(Modified) Gust Measure Results*

To effectively test the gust measure, relatively flat wind profiles are also considered from SUMR-D data in addition to the peak occurrences shown in Fig. 5. This is to provide a good contrast of wind conditions. The (modified) gust measure(s) are calculated for this data-set, tuned using the simulated cases. The tuning parameters for this analysis are as shown in Table III. We define generator speed overshoot $\delta\omega_g$ as the generator speed at the 50 second mark minus the rated generator speed to quantify the severity of the peak:

$$\delta\omega_g = \omega_{g_{t=50}} - \omega_{rated} \tag{11}$$

Fig. 6 shows the results from simulated and field data. The generator speed overshoot is sorted from highest to lowest instances. The gust measure accounting for delay δU_d tracks the severity of the peak fairly well. Specifically, in both simulation and field data plots, it drops off significantly for the flatter wind profiles (which start at index 31). However, it can also be seen, most evidently in the field data plot, that the gust measure underestimates some of the severe generator speed peaks, including the highest two occurrences (at indices 1 and 2). This is due to the

TABLE V: (Modified) Gust Measure(s) Correlation

Measure	Simulation	Field
Gust Measure accounting for delay δU_d (6)	0.8168	0.7884
Modified Gust Measure δG_d (10)	0.8196	0.8936

fact that the gust measure only looks at the wind profile without the knowledge of the proximity of the controller to the critical control transition region. This drawback is remedied by using the modified gust measure. The modified gust measure δG_d is calculated for the same sets of peaks for comparison. As seen in equation (9), a 'Torque Measure' is first calculated to account for proximity of the control to the transition region. It achieves this by penalizing instances that are purely in region 3, with the generator torque at saturation, giving torque measures of zero. With appropriate tuning of the parameters as given in Table III, the modified gust measure boosts instances that are closer to transition and hence likely to be more severe.

In Table V, we evaluate this metric using a simple linear correlation between the assigned measures and the maximum generator speed near the peak occurrence. The advantage of the modified gust measure (10) over the gust measure (6) is most clearly seen in the field data results.

VI. DISCUSSION AND CONCLUSIONS

In this study, we investigated undesirable peaking behavior in wind turbine generator speed transients due to particular gust patterns in the incoming wind. Specifically, that a lull in the wind followed by a positive gust can result in peaks in generator speed and that this can be particularly severe near the control transition region. The SUMR-D wind turbine was chosen for this analysis using simulations for tuning the (modified) gust measure(s) and field data for testing their performance. On filtering and aligning the highest 30 peaks from the SUMR-D simulation and field test data, and taking ensemble means for the nacelle wind speed, generator speed, blade pitch, and generator torque, clear trends can be seen supporting these observations.

Gust Measure [3] analysis was conducted for generator speed peaks of varying severity and a strong correlation of 0.8168 was found for the tuning (simulation) dataset and a correlation of 0.7884 for the testing (field) dataset. As the gust measure only considered the wind speed, a modified gust measure was developed to also take into account the proximity of the controller to the transition region. This transition of the control, from below-rated torque control to above-rated blade pitch control, is more likely to result in generator speed peaks of higher severity under the particular wind gusts that were a focus of this study. The modified gust measure was tuned and tested on the same datasets and was found to be more effective in quantifying the severity of the peaks. By boosting the rating for instances that saw a rapid increase in generator torque, the modified gust measure had a linear correlation of 0.8196 for the tuning (simulation) cases and 0.8936 for the test (field) cases considered.

It can be concluded that the (modified) gust measure(s) can

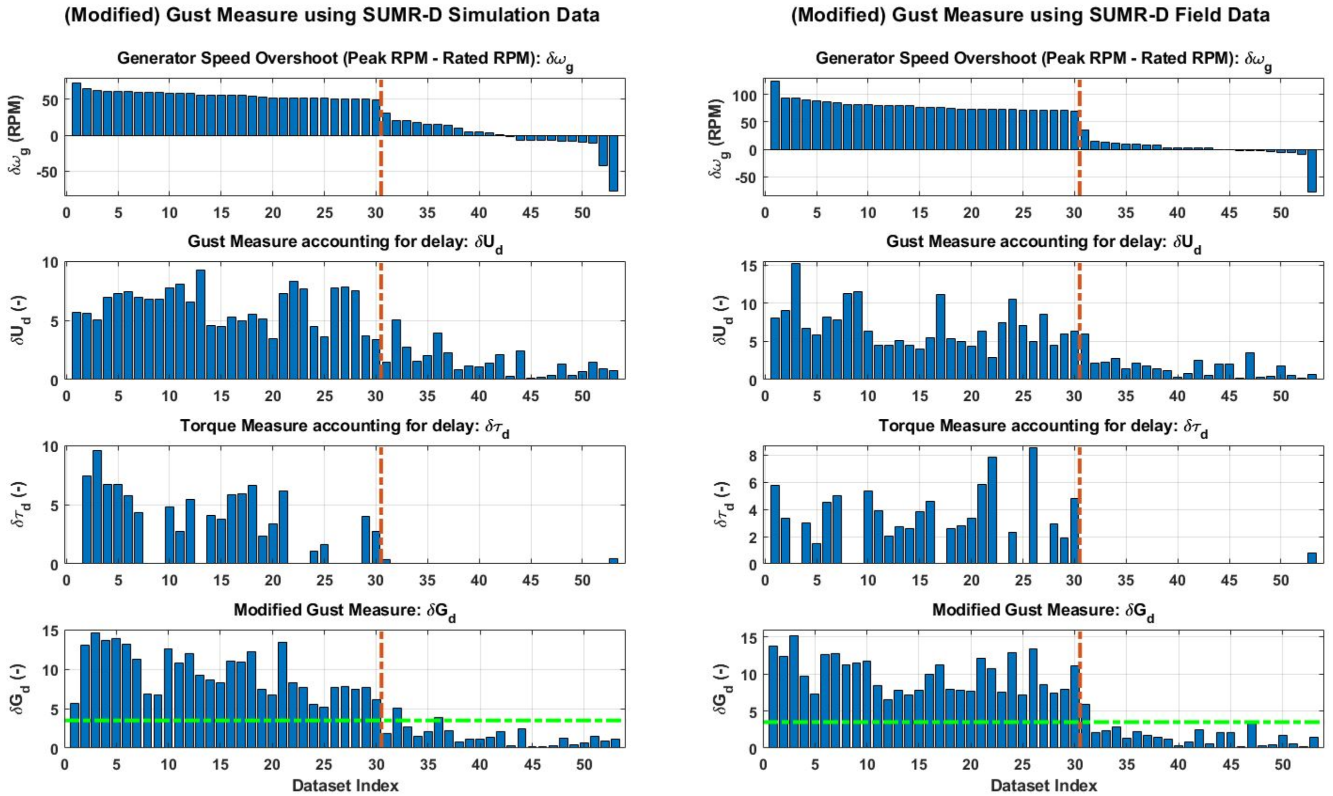

Fig. 6: (Modified) Gust Measure for SUMR-D Simulation (left) and Field (right) datasets. Red dashed lines separate the gust instances from those with flatter wind speed profiles. Green dashed lines denote a proposed modified gust measure threshold of 3.5 above which the probability of the generator speed response peaking would be expected to increase in an online implementation.

be effective tools as online parameters in advanced control techniques to predict and mitigate transients in generator speed. Along with alleviating loads, this can also reduce the probability of an over-speed shutdown event. Since the gust measure [3] has been used in advanced controllers to lead to increased annual energy production (AEP) while maintaining generator speed and structural load constraints [4,19], we anticipate that the modified gust measure may lead to further and more robust performance improvements.

References

[1] L. Y. Pao, K. E. Johnson, “Control of wind turbines,” *IEEE Control Systems Magazine*, 31(2): 44-62, Apr. 2011.

[2] R. Wisniewski, M. Svenstrup, A. S. Pedersen, C. S. Steiniche, “Certificate for safe emergency shutdown of wind turbines,” *Proc. American Control Conf.*, pp. 3667-3672, Jun. 2013.

[3] D. S. Zalkind, “Methods for enabling controls collaboration during wind turbine design,” PhD thesis, University of Colorado, 2020.

[4] D. S. Zalkind, M. M. Nicotra, L. Y. Pao “Constrained power reference control for wind turbines,” *Wind Energy*, Dec. 2021.

[5] M. H. Hansen, L. C. Henriksen, “Basic DTU wind energy controller,” Tech. Rep. E-0018, Technical University of Denmark, 2013.

[6] D. Schlipf, “Controller design and implementation,” TTI GmbH - Sowento TGU, https://www.sowento.com/services/.

[7] D. S. Zalkind, L. Y. Pao, D. P. Martin, K. E. Johnson, “Models used for the simulation and control of a segmented ultralight morphing rotor,” IFAC-PapersOnLine, 50(1): 4478-4483, Jul. 2017.

[8] “Ultra-Large wind turbine,” ARPA-E, https://arpa-e.energy.gov/technologies/projects/ultra-large-wind-turbine

[9] “Segmented Ultralight Morphing Rotor, Demonstrator (SUMR-D),” https://a2e.energy.gov/projects/sumr-d.

[10] L. Y. Pao, D. S. Zalkind, D. T. Griffith, M. Chetan, M. S. Selig, G. K. Ananda, C. J. Bay, T. Stehly, and E. Loth, “Control co-design of 13 MW downwind two-bladed rotors to achieve 25% reduction in levelized cost of wind energy,” *Annual Reviews in Control*, Vol. 51, pp. 331-343, Mar. 2021.

[11] S. Yao, D. T. Griffith, M. Chetan, C. J. Bay, R. Damiani, M. Kaminski, E. Loth, “A gravo-aeroelastically scaled wind turbine rotor at field-prototype scale with strict structural requirements,” *Renewable Energy*, Vol. 156, pp. 535-547 Aug. 2020.

[12] M. Kaminski, E. Loth, D. Zalkind, L. Pao, M. Selig, K. Johnson, “Servo-Aero-Gravo-Elastic (SAGE) scaling of a 13-MW downwind turbine,” *J. Renewable and Sustainable Energy*, 12(6), Nov./Dec. 2020.

[13] C. Bay, R. Damiani, L. Fingersh, S. Hughes, M. Chetan, S. Yao, D. T. Griffith, G. Ananda, M. Selig, D. Zalkind, L. Pao, D. Martin, K. Johnson, M. Kaminski, E. Loth, “Design and testing of a scaled demonstrator turbine at the National Wind Technology Center,” *Proc. AIAA Science and Tech. Forum & Expo*, Jan. 2019.

[14] B. J. Jonkman, “Turbsim user’s guide: version 1.50,” Tech. Rep. NREL/TP-500-46198, National Renewable Energy Laboratory, Golden, CO, Aug. 2009.

[15] https://github.com/OpenFAST/openfast (accessed November 12, 2019)

[16] L. J. Fingersh, K. E. Johnson, “Controls advanced research turbine (CART) commissioning and baseline data collection,” Tech. Rep. NREL/TP-500-32879, National Renewable Energy Laboratory, Golden, CO, Oct. 2002.

[17] E. Loth, L. J. Fingersh, D. T. Griffith, M. Kaminski, C. Qin, “Gravo-aeroelastically scaling for extreme-scale wind turbines,” *Proc. AIAA Applied Aero. Conf.*, AIAA 2017-4215, Jun. 2017.

[18] A. D. Wright, L. J. Fingersh, “Advanced control design for wind turbines; Part I: Control Design, Implementation, and Initial Tests,” Tech. Rep. NREL/TP-500-42437, National Renewable Energy Laboratory, Golden, CO, Mar. 2008.

[19] D. S. Zalkind, L. Y. Pao, ”Constrained wind turbine power control,” *Proc. American Control Conf.*, pp. 3494-3499, Jul. 2019.